

Cite this: *Mater. Adv.*, 2021,
2, 933Received 23rd October 2020,
Accepted 16th December 2020

DOI: 10.1039/d0ma00827c

rsc.li/materials-advances

Improved performance of solution processed OLEDs using *N*-annulated perylene diimide emitters with bulky side-chains†

Sergey V. Dayneko,^{ab} Edward Cieplechowicz,^a Sachin Suresh Bhojgude,^a
Jeffrey F. Van Humbeck,^a Majid Pahlevani^{*c} and Gregory C. Welch^{ib,*a}

We have designed and synthesized three *N*-annulated perylene diimide (PDI) compounds containing sterically bulky alkyl-substituted benzyl moieties (PDI-*X*, where *X* = 1, 2, 3) with photoluminescence quantum yield (PLQY) in the solid-state >20%. The PDI molecules show PLQY of ~0.8 in solution and ~0.2 as neat films. Organic light-emitting diodes (OLEDs) have been fabricated using these new PDI molecules as light emitters with the active layer being solution processed from non-halogenated solvents. The OLED devices had brightness of ~2000 cd m⁻² and low turn-on voltage of ~3 V, among the best for PDI based red colored OLEDs.

Perylene diimide (PDI) based materials have been actively explored in the context of fluorescence labels,¹ organic semiconducting devices,^{2,3} and light harvesters.^{4,5} The PDI chromophore has key properties such as tunable photon absorption and emission in the visible region, high photothermal stability, and solution processability.⁶ The high photoluminescence quantum yield (PLQY) of light-emitting materials in the solid-state, excellent electron and hole transport capacity, good film-forming properties and colour purities are considered essential parameters for the development of high-performance organic light-emitting diodes (OLEDs).⁷ PDI materials with PLQY of close to 100% in solution^{8,9} have been reported but the PLQY in solid-state is generally low due to aggregation-caused quenching (ACQ).¹⁰

Efforts have been made to increase the PLQY of PDI materials in the solid-state. Zhang and coworkers synthesized PDI molecules with bulky di-*tert*-butylphenyl and trityl moieties enabling PLQY near 30% in neat films and an optical quantum efficiency of 54% for luminescent solar concentrators incorporating these

molecules.⁴ Kozma and coworkers appended large naphthyl moieties to the PDI chromophore and were able to achieve PLQY ~ 23% in neat films and developed OLEDs based on these materials with moderate external quantum efficiency (EQE) of 0.6%.¹¹ The performance of OLEDs depends not only on the PLQY of the emitting layer but charge transport, radiative exciton formation efficiency, and light outcoupling efficiency,¹² thus completely isolating the PDI chromophore is not a option. A way to increase PLQY without sacrificing electrical performance is to control the aggregation of the PDI units *via* the formation of dimers, trimers, tetramers.¹³ Such larger oligomers and/or starburst derivatives can reduce co-facial π - π stacking and limit ACQ.¹⁴

Recently, the Welch group has reported on a series of *N*-annulated PDI dimers with controlled aggregation tendencies¹⁵ and green solvent processability¹⁶ that have found utility in both organic solar cells¹⁷⁻²⁰ and OLEDs.^{21,22} These compounds are readily made on scale, are highly soluble in common organic processing solvents, and exhibit a range of optoelectronic properties. *N*-Annulation destabilizes the frontier molecular orbital energy levels changing the PDI electronic structure²³ while the pyrrolic *N*-position can be readily functionalized.²⁴ We have shown that an *N*-annulated PDI dimer with bulky 2-ethylhexyl sidechains (tPDI₂N-EH) can function as an effective light emitter in OLEDs²¹ and our hypothesis was that increasing the bulk of the side-chain would lead to greater PLQY in the film and subsequent increased OLED device performance.

Herein, we report the synthesis and characterisation of air stable red-light-emitting *N*-annulated PDI dimers substituted at pyrrolic *N*-atom position with 2,4,6-trimethylbenzyl, 2,4,6-trisopropylbenzyl, and 3,5-di-*tert*-butylbenzyl side-chains. The target structures tPDI₂N-trimethylbenzyl (PDI-1), tPDI₂N-trisopropylbenzyl (PDI-2), and tPDI₂N-di-*tert*-butylbenzyl (PDI-3) are shown in Fig. 1. The benzyl side chains with sterically bulky alkyl substituents can lead to different intermolecular interactions as compared to alkyl side chains, with the possibility of different electronic influences on the dimeric PDI core. The PDI

^a Department of Chemistry, University of Calgary, 731 Campus Place NW, Calgary, Alberta, T2N 1N4, Canada. E-mail: gregory.welch@ucalgary.ca

^b Genoptic LED Inc., 6000 72nd Avenue SE, Calgary, AB, T2C 5G3, Canada

^c Department of Electrical and Computer Engineering, Queen's University, 19 Union St., Kingston, ON, K7L 3N6, Canada.
E-mail: majid.pahlevani@queensu.ca

† Electronic supplementary information (ESI) available. See DOI: 10.1039/d0ma00827c



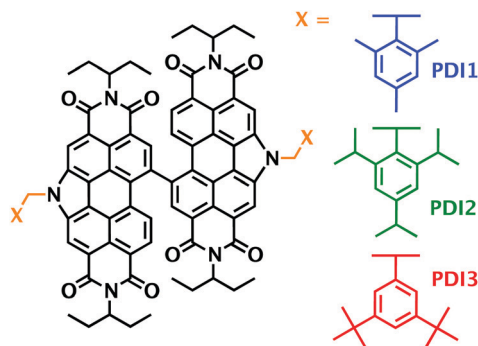


Fig. 1 Chemical structures of the three new PDI molecules designed, synthesized, and used as light emitters in OLED devices.

dimers are easily processed into uniform films from non-halogenated solvents. The UV-vis absorption and PL spectra of the PDI molecules in diluted solution were recorded and PLQYs were calculated. The absolute PLQY of PDI molecules dispersed into neat films were measured by an integrating sphere. Finally, OLED devices based on the emitting layer containing the PDI-X ($X = 1, 2, 3$) molecules were fabricated and tested in air. The OLED devices reported here show enhanced performance compared to previously reported PDI dimers.^{21,22} Complete synthesis and characterization are presented in the ESI.†

To investigate the influence of different substituted benzyl side chains on the photophysical properties of the PDI derivatives, the UV-vis absorption and emission spectra of PDI-1, PDI-2 and PDI-3 in *o*-xylene solution and as thin films were measured (Fig. 2 and Table 1). In the *o*-xylene solution, the absorption spectra of all PDI molecules are identical and demonstrate the two characteristic maxima of the PDI chromophore.^{25–27} All dimers have high PLQY of ~ 0.7 in solution with similar PL spectra and emission maxima at ~ 580 nm. The high PLQY of these compounds is attributed to the bulky-side chains which inhibits aggregation resulting in partial isolation of PDI dimer core.^{24,28,29} For films cast from *o*-xylene, the absorption spectra of all PDI molecules are slightly red-shifted and broadened compared to the solution indicating that the PDI dimers are weakly aggregated. All PDI molecules in the film have PLQY of 20–25% which is high for PDI-based light emitting materials.

A multi-stack device structure was used to fabricated OLEDs³¹ (Fig. 3). The substrate was glass and indium tin oxide

Table 1 Optical data for PDI 1–3 in solution and as neat films

| | | Absorption (nm) | | Emission (nm) | | Stokes shift ^c (cm ⁻¹) | PLQY (%) |
|-------|-----------------------|--------------------|-----|---------------|-----|---|----------|
| | | Onset ^b | 0–0 | 0–1 | Max | | |
| PDI-1 | Solution ^a | 543 | 530 | 495 | 586 | 84 | 76 |
| | Film ^a | 564 | 535 | 496 | 640 | 97 | 20 |
| PDI-2 | Solution ^a | 543 | 530 | 493 | 591 | 90 | 65 |
| | Film ^a | 584 | 532 | 494 | 642 | 101 | 25 |
| PDI-3 | Solution ^a | 546 | 532 | 494 | 584 | 76 | 74 |
| | Film ^a | 572 | 532 | 494 | 650 | 83 | 25 |

^a Solution and neat films of PDI 1–3 in *o*-xylene or spin-cast from *o*-xylene. ^b Absorption onset determined from the intersection of optical absorption and emission spectra. ^c Stokes Shift ($\Delta\nu = \nu_{\max,PL} - \nu_{\max,ABS}$).³⁰ ^d FWHM: full width at half maximum of photoluminescence spectra.

(ITO) was used as the anode. Poly(3,4-ethylenedioxythiophene):poly(4-styrenesulfonic acid) (PEDOT:PSS) and polyvinylcarbazole (PVK) were used as the hole injection and transport layers, respectively. Zinc oxide (ZnO) was used as an electronic transport layer with silver (Ag) as the top cathode. The PDI molecules were used individually in the emitting layer in combination with the polyfluorene polymer PFO (*i.e.* poly(9,9-di-*n*-octylfluorenyl-2,7-diyl)) to assist with hole transport.²¹

PEDOT:PSS films were formed by spin-casting aqueous suspension of PEDOT:PSS on top of cleaned glass/ITO and then annealed at 150 °C for 30 min in air. PVK was spin-coated from toluene on top of the PEDOT:PSS and annealed at 120 °C. Of note the PVK film is resistant to *o*-xylene solvent and thus allows for good formation of the emitting layer films on top.²² The emitter layer was spin-coated on top of the PVK film from *o*-xylene solutions of PFO:PDI molecules (1:9 w/w ratio). ZnO nanoparticles in methanol were spin-coated on top and annealed at 60 °C for 30 min in air. The emitting layer films were found to show good tolerance to methanol solvent (Fig. S1 and S2, ESI†). The Ag top electrode deposited *via* thermal evaporation (Fig. 3).

The device parameters of PDI-based OLEDs are summarized in Table 2. All PDI-based OLEDs had similar performance with a maximum external quantum efficiency (EQE) of $\sim 0.7\%$, luminous efficiency (LE) of 0.6 cd A⁻¹, power efficiency (PE) of ~ 0.3 lm W⁻¹ and a maximum of luminous (L_{\max}) of 2400 cd m⁻²

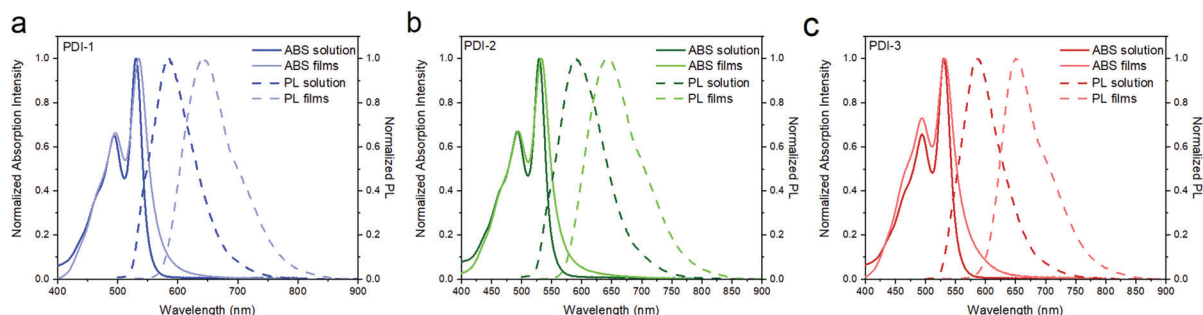


Fig. 2 Absorption (ABS) and emission (PL) spectra of all PDI molecules in *o*-xylene solutions and neat films processed from *o*-xylene solutions.



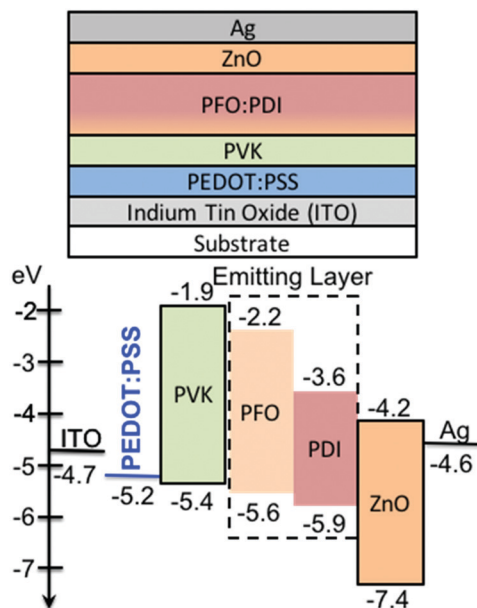


Fig. 3 Structure of the PDI-based OLEDs and electronic energy levels.

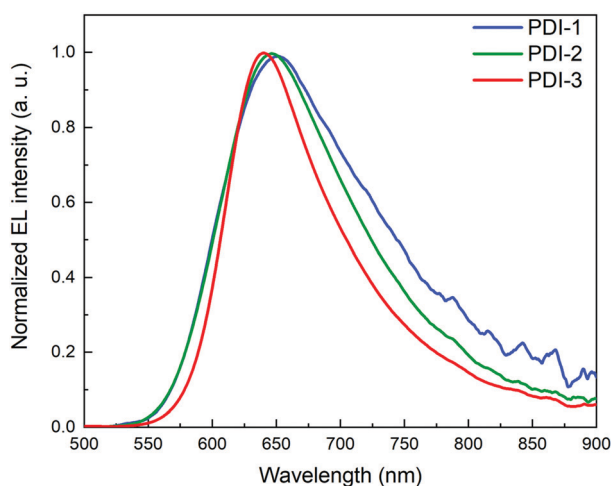


Fig. 4 Electroluminescence spectra of the PDI-1, PDI-2, PDI-3 under external voltage.

Table 2 OLED device parameters performance based on PFO:PDI molecule emitting layers

| Emitter ^a | V_{on} ^b (V) | EQE_{max} ^c (%) | LE_{max} ^d ($cd A^{-1}$) | PE_{max} ^e ($lm W^{-1}$) | L_{max} ^f ($cd m^{-2}$) |
|-------------------------|------------------------------|---------------------------------|--|--|---|
| PDI-1 | 3.2 | 0.4 | 0.36 | 0.22 | 1800 |
| PDI-2 | 3.8 | 0.7 | 0.58 | 0.29 | 2145 |
| PDI-3 | 3.3 | 0.64 | 0.62 | 0.30 | 2400 |
| tPDI2N-EH ²¹ | 2.6 | 0.06 | 0.05 | 0.03 | 400 |

^a Blended with PFO (ratio of 18:2 PFO:PDI). ^b Turn on voltage was determined at the brightness of $1 cd m^{-2}$. ^c EQE – external quantum efficiency. ^d LE – luminous efficiency. ^e PE – power efficiency. ^f L_{max} – maximum of luminance.

and low turn-on voltage (V_{on}) of ~ 3 V. Notably, the electroluminescence (EL) spectra of all PDI molecules are similar with a deep red maximum at ~ 650 nm with the CIE (international commission on illumination) coordinates of ($x = 0.66$; $y = 0.33$) (Fig. 4). The EQE is a critical parameter of a OLED device that describes the ratio between the number of emitted photons and injected charge carriers which has been expressed by equation $EQE = \gamma \cdot \eta_{s/T} \cdot q \cdot \eta_{out}$,^{32–35} where γ is the charge carrier balance factor; $\eta_{s/T}$ is the singlet–triplet factor; q is the effective quantum yield of the emitter material and η_{out} is the out-coupling efficiency of the emitted light. For theoretical evaluation of EQE the γ value is often assumed to be unity, $\eta_{s/T}$ equal 0.25 for fluorescent emitters, q equals the PLQY of EL not considering the emitting dipole orientation factor and the Purcell effect;³⁶ η_{out} can be estimated as $1/(2n^2)$ for isotropic emitters, where n is the refractive index of the organic EL.³⁷ Here, the theoretical EQE is estimated at 1% based on a 20% PLQY and $n \sim 1.5$.³⁸ The OLED devices had a maximum EQE ranging from 0.4% to 0.7% for each different PDI molecule. Clearly by varying the sidechain of the PDI molecule, slight changes in OLED device performance are obtained. Compared to the literature these PDI based OLEDs have much improved performance.^{11,12}

Conclusion

A series of *N*-annulated perylene diimides with sterically bulky alkyl-substituted benzyl side chains were designed, synthesized, and used as emitters in OLED devices. These PDI dimers demonstrated high PLQY in the solution ($\sim 80\%$) and as neat films ($\sim 20\%$). The PDI molecules were used as emitting layers and solution processed from the non-halogenated solvent *o*-xylene. All OLED devices based on the PDI molecules showed good performance with EQE $\sim 0.7\%$, high brightness of $2400 cd m^{-2}$ with deep red maximum EL spectra of ~ 650 nm, and CIE coordinates of ($x = 0.66$; $y = 0.33$). Future work is set to explore the utility of such molecules in complete roll-to-roll processed OLED devices.

Conflicts of interest

There are no conflicts to declare.

Acknowledgements

All authors thank Alberta Innovates (grant # G2018000901) for funding. SVD would also like to thank the MITACS Accelerate and Elevate Post-Doctoral Programs and Geoptics LED Inc. for salary support.

References

- 1 K. Huth, M. Glaeske, K. Achazi, G. Gordeev, S. Kumar, R. Arenal, S. K. Sharma, M. Adeli, A. Setaro, S. Reich and R. Haag, *Small*, 2018, **14**, 1800796.
- 2 G. Zhang, J. Zhao, P. C. Y. Chow, K. Jiang, J. Zhang, Z. Zhu, J. Zhang, F. Huang and H. Yan, *Chem. Rev.*, 2018, **118**, 3447–3507.



- 3 A. Wadsworth, M. Moser, A. Marks, M. S. Little, N. Gasparini, C. J. Brabec, D. Baran and I. McCulloch, *Chem. Soc. Rev.*, 2019, **48**, 1596–1625.
- 4 B. Zhang, H. Soleimaninejad, D. J. Jones, J. M. White, K. P. Ghiggino, T. A. Smith and W. W. H. Wong, *Chem. Mater.*, 2017, **29**, 8395–8403.
- 5 C. Haines, M. Chen and K. P. Ghiggino, *Sol. Energy Mater. Sol. Cells*, 2012, **105**, 287–292.
- 6 B. Lü, Y. Chen, P. Li, B. Wang, K. Müllen and M. Yin, *Nat. Commun.*, 2019, **10**, 767.
- 7 B. Geffroy, P. le Roy and C. Prat, *Polym. Int.*, 2006, **55**, 572–582.
- 8 F. Würthner, C. R. Saha-Möller, B. Fimmel, S. Ogi, P. Leowanawat and D. Schmidt, *Chem. Rev.*, 2016, **116**, 962–1052.
- 9 F. Würthner, *Chem. Commun.*, 2004, 1564–1579.
- 10 F. Zhang, Y. Ma, Y. Chi, H. Yu, Y. Li, T. Jiang, X. Wei and J. Shi, *Sci. Rep.*, 2018, **8**, 8208.
- 11 E. Kozma, W. Mróz, F. Villafiorita-Monteleone, F. Galeotti, A. Andicsová-Eckstein, M. Catellani and C. Botta, *RSC Adv.*, 2016, **6**, 61175–61179.
- 12 Y. Qin, G. Li, T. Qi and H. Huang, *Mater. Chem. Front.*, 2020, **4**, 1554–1568.
- 13 M. Li, H. Yin and G.-Y. Sun, *Appl. Mater. Today*, 2020, **21**, 100799.
- 14 H. Hu, Y. Li, J. Zhang, Z. Peng, L. Ma, J. Xin, J. Huang, T. Ma, K. Jiang, G. Zhang, W. Ma, H. Ade and H. Yan, *Adv. Energy Mater.*, 2018, **8**, 1800234.
- 15 F. Tintori, A. Laventure and G. C. Welch, *Soft Matter*, 2019, **15**, 5138–5146.
- 16 C. R. Harding, J. Cann, A. Laventure, M. Sadeghianlemraski, M. Abd-Ellah, K. R. Rao, B. S. Gelfand, H. Aziz, L. Kaake, C. Risiko and G. C. Welch, *Mater. Horiz.*, 2020, **7**, 2959–2969.
- 17 F. Tintori, A. Laventure, J. D. B. Koenig and G. C. Welch, *J. Mater. Chem. C*, 2020, **8**, 13430–13438.
- 18 S. V. Dayneko, A. D. Hendsbee, J. R. Cann, C. Cabanetos and G. C. Welch, *New J. Chem.*, 2019, **43**, 10442–10448.
- 19 M. Nazari, M. Martell, T. A. Welsh, O. Melville, Z. Li, J. Cann, E. Cieplechowicz, Y. Zou, B. H. Lessard and G. C. Welch, *Mater. Chem. Front.*, 2018, **2**, 2272–2276.
- 20 S. V. Dayneko, A. D. Hendsbee and G. C. Welch, *Chem. Commun.*, 2017, **53**, 1164–1167.
- 21 S. V. Dayneko, M. Rahmati, M. Pahlevani and G. C. Welch, *J. Mater. Chem. C*, 2020, **8**, 2314–2319.
- 22 M. Rahmati, S. V. Dayneko, M. Pahlevani and G. C. Welch, *ACS Appl. Electron. Mater.*, 2020, **2**, 48–55.
- 23 M. Nazari, E. Cieplechowicz, T. A. Welsh and G. C. Welch, *New J. Chem.*, 2019, **43**, 5187–5195.
- 24 S. V. Dayneko, A. D. Hendsbee and G. C. Welch, *Small Methods*, 2018, **2**, 1800081.
- 25 W. E. Ford, *J. Photochem.*, 1986, **34**, 43–54.
- 26 W. E. Ford and P. V. Kamat, *J. Phys. Chem.*, 1987, **91**, 6373–6380.
- 27 J. Cann, S. Dayneko, J.-P. Sun, A. D. Hendsbee, I. G. Hill and G. C. Welch, *J. Mater. Chem. C*, 2017, **5**, 2074–2083.
- 28 C. Huang, S. Barlow and S. R. Marder, *J. Org. Chem.*, 2011, **76**, 2386–2407.
- 29 A. Reisch and A. S. Klymchenko, *Small*, 2016, **12**, 1968–1992.
- 30 B. Valeur and M. N. Berberan-Santos, *Molecular Fluorescence*, Wiley-VCH Verlag GmbH & Co. KGaA, Weinheim, Germany, 2012.
- 31 S. B. Meier, D. Tordera, A. Pertegás, C. Roldán-Carmona, E. Ortí and H. J. Bolink, *Mater. Today*, 2014, **17**, 217–223.
- 32 T. Tsutsui, E. Aminaka, C. P. Lin and D.-U. Kim, *Philos. Trans. R. Soc. London, Ser. A*, 1997, **355**, 801–814.
- 33 S.-Y. Kim, W.-I. Jeong, C. Mayr, Y.-S. Park, K.-H. Kim, J.-H. Lee, C.-K. Moon, W. Brütting and J.-J. Kim, *Adv. Funct. Mater.*, 2013, **23**, 3896–3900.
- 34 B. Sim, C.-K. Moon, K.-H. Kim and J.-J. Kim, *ACS Appl. Mater. Interfaces*, 2016, **8**, 33010–33018.
- 35 W. Brütting, J. Frischeisen, T. D. Schmidt, B. J. Scholz and C. Mayr, *Phys. Status Solidi*, 2013, **210**, 44–65.
- 36 E. M. Purcell, H. C. Torrey and R. V. Pound, *Phys. Rev.*, 1946, **69**, 37–38.
- 37 N. C. Greenham, R. H. Friend and D. D. C. Bradley, *Adv. Mater.*, 1994, **6**, 491–494.
- 38 Z. Kışınçı, Ö. F. Yüksel and M. Kuş, *Synth. Met.*, 2014, **194**, 193–197.

